ADVANCES IN ATMOSPHERIC SCIENCES, VOL. 29, NO. 2, 2012, 285–294

Observational Evidence for the Monin-Obukhov Similarity under All Stability Conditions

NIU Shengjie* (牛生杰), ZHAO Lijuan (赵丽娟), LU Chunsong (陆春松), YANG Jun (杨 军), WANG Jing (王 静), and WANG Weiwei (王巍巍)

Key Laboratory of Meteorological Disaster of Ministry of Education, School of Atmospheric Physics, Nanjing University of Information Science and Technology, Nanjing 210044

(Received 11 July 2011; revised 20 September 2011)

ABSTRACT

Data collected in the surface layer in a northern suburban area of Nanjing from 15 November to 29 December 2007 were analyzed to examine the Monin-Obukhov similarity for describing the turbulent fluctuations of 3D winds under all stability conditions and to obtain the turbulence characteristics under different weather conditions. The results show that the dimensionless standard deviations of turbulent velocity components (σ_u/u_*, σ_v/u_*, σ_w/u_*) and dimensionless turbulent kinetic energy (TKE) can be well described by "1/3" power law relationships under stable, neutral, and unstable conditions, with $\sigma_u/u_* > \sigma_v/u_* > \sigma_w/u_*$. Land use and land cover changes mainly impact dimensionless standard deviations of horizontal component fluctuations, but they have very little on those of the vertical component. The dimensionless standard deviations of wind components and dimensionless TKE are remarkably affected by different weather conditions; the deviations of horizontal wind component and dimensionless TKE present fog day > clear sky > overcast > cloudy; the trend of the vertical wind component is the reverse. The surface drag coefficient at a Nanjing suburban measurement site during the observation period was obviously higher than at other reported plains and plateau areas, and was approximately one order larger in magnitude than the reported plains areas. Dimensionless standard deviation of temperature declined with increasing $|z'/L|$ with an approximate "$-1/3$" slope in unstable stratification and "$-2/3$" slope in stable stratification.

Key words: Monin-Obukhov similarity theory, boundary stability, boundary layer parameterization

Citation: Niu, S. J., L. J. Zhao, C. S. Lu, J. Yang, J. Wang, and W. W. Wang, 2012: Observational evidence for the Monin-Obukhov similarity under all stability conditions. *Adv. Atmos. Sci.*, **29**(2), 285–294, doi: 10.1007/s00376-011-1112-6.

1. Introduction

Since Monin and Obukhov (1954) proposed the boundary layer similarity theory (M-O similarity hereafter), the M-O similarity has been extensively investigated under unstable stability; however, progress under stable stratification has been relatively slow (Caughey et al., 1979; Nieuwstadt, 1984a, b; Smedman, 1988; Dias et al., 1995; Dias and Brutsaert, 1996; Forrer and Rotach, 1997; Howell and Sun, 1999; Mahrt, 1999). Carson and Richards (1978) suggested that the formulation of Hicks (1976) is the most compatible to modeling the surface turbulent fluxes of the stable boundary layer. Simpson et al. (1998) validated that the M-O similarity can be used within the roughness sublayer. Pahlow et al. (2001) investigated the applicability of the M-O similarity for stable conditions, based the measurements from several field experiments. Using the data collected in the Cooperative Atmosphere-Surface Exchange Study-99 (CASES-99), the M-O similarity function of the dissipation rate of turbulent kinetic energy and the structure parameter of temperature were determined (Hartogensis and De Bruin, 2005). Cheng et al. (2005) investigated the performance of the M-O similarity in the stable nocturnal boundary layer during the CASES-99 and found that the M-O similarity holds when a new equilibrium is reached or recovered, especially during the entire process of the nonbreaking internal gravity waves and the well-developed stages both of the density current

*Corresponding author: NIU Shengjie, niusj@nuist.edu.cn

and of the low-level jet. Zilitinkevich and Esau (2007) revised the similarity for the stably stratified atmospheric boundary layer and gave an analytical formulation for the wind velocity and potential temperature profiles. Foken (2006) reviewed the development of the M-O similarity in the past 50 years, and proposed that the application of the Monin-Obukhov Similarity Theory is limited to the surface layer above the roughness sublayer, to a range of $|z/L| \leqslant 1 \sim 2$, and over homogeneous surfaces.

Due to the great importance of the turbulence structure under stable atmospheric conditions for application in air pollution, heat and momentum calculations, and numerical modeling of the boundary layer, it is necessary to devote more effort to studying the turbulence structure in a stable atmospheric stratification.

Furthermore, urban agglomeration and human activities remarkably impact the dynamic and thermodynamic processes in urban boundary layers (Martilli, 2002). Expansion of urban environments has increased common concern from social communities. Researchers have performed field experiments (Rotach, 1995; Grimmond and Oke, 1999; Wilson et al., 2002; Hammerle et al., 2007; Hiller et al., 2008) and modeling studies (Masson et al., 2002; Grimmond and Oke, 2002) and have discussed the characteristics of eddy kinetic energy in the urban boundary layer and the energy budget. However, due to the scarcity of measurements and the complexity of turbulence motion in the boundary layer and differences among cities, many issues regarding interactions between the urban underlying surface and the boundary layer have remained elusive.

Additionally, accurate depiction of the standard deviations of turbulent velocity components is required for the modeling of the dispersion of air pollutants in the planetary boundary layer (PBL). The behavior of dimensionless standard deviations of turbulent velocity components under unstable (Kaimal et al., 1976; Panofsky et al., 1977) and neutral (Deardorff, 1970) conditions has been well established; however, no obvious conclusion has been revealed about the behavior of dimensionless standard deviations of turbulent velocity components in the stable boundary layer (Sorbjan, 1987; Sharan and Gopalakrishnan, 1999). And the PBL parameterization not only plays a critical role in simulating the heat, moment, and moisture exchange in the boundary layer, but it also has an important influence on climate studies (Argüeso et al., 2011) and simulations of tropical cyclones (Braun and Tao, 2000; Srinivas et al., 2007; Hill and Lackmann, 2009). Thus, effort still needs to be focused on the behavior of turbulent motion in the boundary layer, especially under stable conditions.

Despite the progress, our understanding of turbulence over suburban areas under different stabilities and weather conditions is still far from complete because of the complexity of turbulent motion. Nanjing lies in the western part of the Changjiang Delta and is one of the high-frequency areas for winter fog. In this study, we focused on two objectives: (1) to examine the M-O similarity for describing the turbulent fluctuations of 3D winds under all stability conditions over suburban areas to provide a basis for boundary-layer modeling and parameterizations, (2) to analyze the turbulence characteristics under different weather conditions to provide a basis for studies on the formation and dissipation of fogs and the diffusion of atmospheric pollutants.

2. Experiment, data, and analysis

2.1 *Site description and instrumentation*

A field-observation experiment examining the boundary-layer atmosphere was conducted at a site in Nanjing University of Information Science and Technology (NUIST) from 15 November to 29 December 2007, the site is a flat at ∼25 m above sea level, open, suburban grassland area with sparse buildings and trees located ∼20 km north of Nanjing City, and this area is representative of Nanjing suburban areas.

A three-dimensional (3D) sonic anemometer-thermometer instrument (CSAT3, Campbell, USA) was used in the experiment to measure the fluctuations of three directional velocity components (u, v, w) and acoustic virtual temperature. A LiCor7500 gas analyzer (LiCor Inc, USA) was used to measure the fluctuations of CO_2 and moisture. The instruments were mounted at 2.0 m above ground level (median roughness length $z_0 = 0.02$ m), giving a relatively small footprint. The measurements were sampled at 10 Hz, and data were stored in a Data Logger CR5000 (Campbell, USA): a total of 37 975 800 groups of samples were acquired.

Additionally, we ran an EnviroStation (ICT International Pty Ltd, Australia) during the same period in which eddy-covariance (EC) measurements were performed. The station was equipped with the following sensors: air temperature (TA) and relative humidity sensors (HU), solar radiation sensor (SR2), photosynthetically active radiation sensor (PR1), anemometer (AN2), wind direction sensor (WD2/3), and barometer (BP). All variables were measured in 1-s intervals and afterward were averaged to 1-min values, which were then stored on a smart logger (SL5-1L).

2.2 *Data analysis*

The quality control of raw observational data was similar to that of Vickers and Mahrt (1997). First, data spikes in the raw data were removed. The local averaging scale was chosen to be 5 min, then we computed the mean and standard deviation for a series of moving windows of 5 min. The window moved one point at a time through the series. If the difference between a point and the 5-min average was > 3.5 standard deviations, the point was considered a spike and was replaced using linear interpolation between data points. When four or more consecutive points were detected, they were not considered as spikes and were not replaced. This process was repeated until no spikes remained. Second, for 30-min observation, if the total number of spikes replaced exceeded 1% of the total number of data points, the data during this period was removed. Third, the data during periods with precipitation, before and right after rainfall within an hour, were also removed. Then the skewness and kurtosis of each variable were computed for every 30 min of data. When the skewness was outside the range (−3.6, 3.6) or the kurtosis was >10 for the 30-min data, the 30-min data were removed.

According to Foken and Wichura (1996), the stationary coefficient (Δst) and the integral turbulence characteristics coefficient (ITC) were used to assess the fulfillment of the theoretical requirements for representative EC measurements. The stationary coefficient (Δst) was defined as the relative deviation between the 30-min flux value of each component and the respective average of the 5-min flux values for the same period. The integral turbulence characteristics coefficient (ITC) was defined as the relative deviation between the measured and theoretical flux-variance similarity (σ_w/u_*), which was estimated by an empirical model using the Monin-Obukhov length. For these two parameters, while the values were <30%, the measurement was tagged as high-quality data. Measurements with the values of 30%–100% were flagged as being of good quality, whereas measurements with the values of >100% were not considered to meet the requirements.

After quality control, the data from the eddy-covariance system were processed using the Planner-Fit method (Wang et al., 2007), and the turbulent parameters and fluxes were calculated following the rules of Reynolds' averaging (Stull, 1988). Then the difference of the measurements between the sonic anemometer and the weather station were calculated. If the difference of air temperature and water vapor concentration exceeded 5°C and 100 mmol m^{-3}, the data from the sonic anemometer were removed (Hiller et al., 2008). The last steps were the damping loss correction (Eugster and Senn, 1995) and the Webb correction (Webb et al., 1980) for the flux data.

3. Results

3.1 *Standard deviations of turbulent velocity*

According to classical M-O similarity theory, the dimensionless standard deviations of velocity components σ_i/u_* ($i = u,\ v,\ w$) in the surface layer in unstable stratification should be functions of only the dimensionless length scale z'/L, given by the so-called "1/3" power-law (Panofsky et al., 1977)

$$\frac{\sigma_i}{u_*} = A\left(1 - B\frac{z-d}{L}\right)^{\frac{1}{3}} = A\left(1 - B\frac{z'}{L}\right)^{\frac{1}{3}}, \quad i = u, v, w, \tag{1}$$

where A and B are empirical coefficients,

$$L \equiv \frac{-u_*^3}{k(g/T_{\rm v})(\overline{w'\theta'})_{\rm s}}$$

is the Monin-Obukhov length, g is the acceleration due to gravity, $T_{\rm v}$ is the virtual temperature, the subscript s denotes at the surface, $z' = z - d$ is the adjusted height that takes into account the surface roughness length, z is the height above the surface, and $d = 0.02$ is dynamic zero displacement.

The preprocessed data were used to calculate the dimensionless standard deviations of velocity components in the northern suburban area of Nanjing in different stratifications; the results are plotted in Fig. 1. The results show that the dimensionless standard deviations of velocity components basically do not change with stability when $|z'/L| < 0.1$, and they follow the 1/3 power law when$|z'/L| > 1$. And the optimum similarity functions of σ_u/u_*, σ_v/u_*, and σ_w/u_* are as follows:

$$\begin{cases} \sigma_u/u_* = 3.73\,(1 + 3.39z'/L)^{1/3} \\ \sigma_v/u_* = 3.49\,(1 + 1.86z'/L)^{1/3} \\ \sigma_w/u_* = 1.62\,(1 + 0.25z'/L)^{1/3} \end{cases}, \ z'/L > 0\,, \tag{2a}$$

$$\begin{cases} \sigma_u/u_* = 3.73\,(1 - 3.78z'/L)^{1/3} \\ \sigma_v/u_* = 3.49\,(1 - 3.12z'/L)^{1/3} \\ \sigma_w/u_* = 1.62\,(1 - 0.15z'/L)^{1/3} \end{cases}, \ z'/L < 0\,. \tag{2b}$$

The scatter may arise from the impacts of local terrain (including buildings, etc.) and low-frequency eddies on horizontal wind component fluctuations (Liu et al., 2002). From Fig. 1 it can be seen that under unstable and stable conditions the σ_w/u_* changes are very small with stability and can be regarded as an approximate constant, which is similar to the conclusion of Panofsky and Dutton (1984) that under a stable stratification condition.

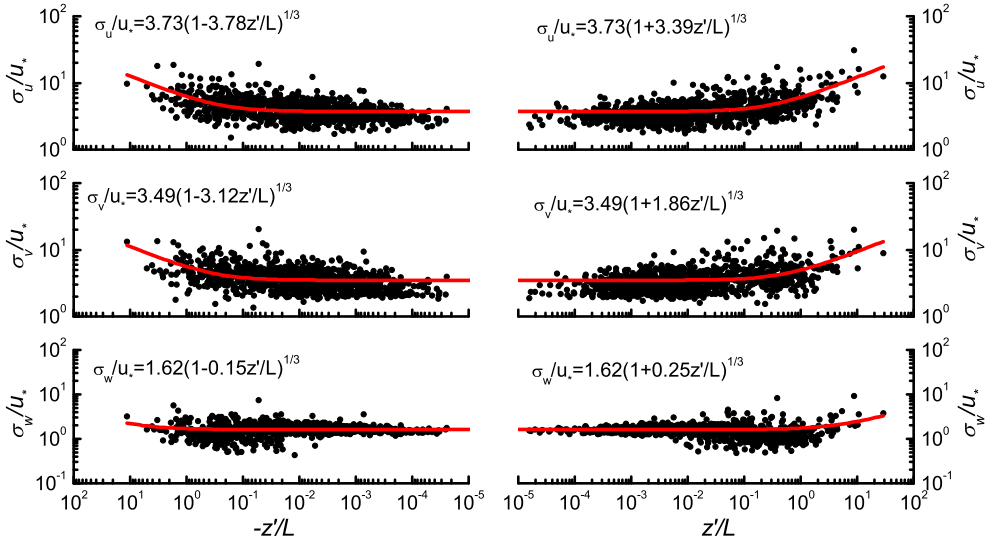

Fig. 1. Dimensionless standard deviations of velocity components σ_i/u_* ($i = u,v,w$) as a function of z'/L.

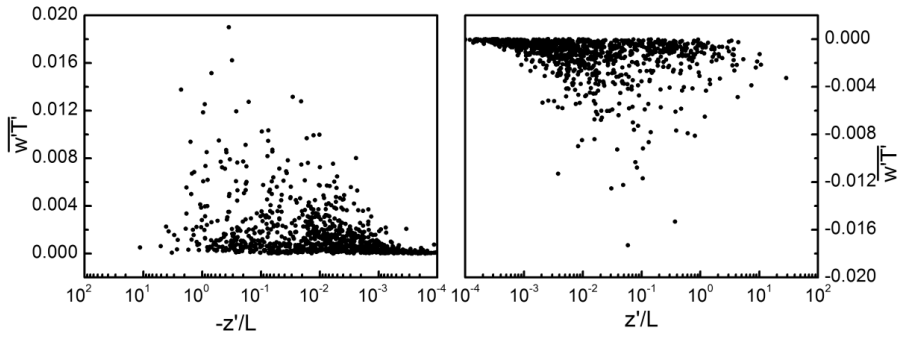

Fig. 2. Turbulence heat flux $\overline{w'T'}$ as a function of z'/L.

Figure 2 shows the variation of $\overline{w'T'}$ with stability (z'/L). $\overline{w'T'}$ and z'/L in stable stratification exhibit a down pointing triangle distribution, i.e., $\overline{w'T'}$ decreased when the stability gradually increases from the near-neutral stratification, but after z'/L>0.1, it increased with increasing stability (Fig. 2b). However, in an unstable stratification $\overline{w'T'}$ and z'/L display an upward pointing triangle distribution, i.e., $\overline{w'T'}$ increased with decreasing stability at first, after z'/L<−0.1, it decreased with decreasing stability (Fig. 2a).

Based on Figs. 1 and 2, we divided turbulent motions in the boundary layer into three stability regimes: a stable regime (z'/L>0.1) wherein intermittent turbulences, meandering motions, and wave motions occur, "nonturbulent" motions develop, and dimensionless standard deviations of wind components increase with increasing stability; an unstable regime (z'/L<−0.1), with stability decreasing, convection beginning to develop, velocity of the air movement becoming stronger; and a near-neutral regime ($-0.1 \leqslant z'/L \leqslant 0.1$) wherein the turbulent motion is mostly mechanically generated and appears to be in a classic state of turbulence and the similarity law is applicable. Notably, the different values of z'/L that divided the stratification were used by other researchers [e.g., z'/L= 0.02 in Malhi (1995), and z'/L= 0.06 in Mahrt et al. (1998)].

Table 1 gives dimensionless standard deviations of velocity components in near-neutral stratification (taken as $-0.1 \leqslant z'/L \leqslant 0.1$ in this study) for different areas. From Table 1 it can be seen that the general trend of the dimensionless standard deviations over different underlying surfaces in the Nanjing region is $\sigma_u/u_* > \sigma_v/u_* > \sigma_w/u_*$. The values of dimensionless standard deviations of horizontal velocity components are obviously larger than those in other reported cities in China and those over the flat terrains in other reported counties; the value of σ_w/u_* is slightly larger than those in other reported places. Therefore, the

Table 1. Dimensionless standard deviations of velocity components in near-neutral stratification for different areas.

Site (source)	Underlying surface	Observing time	σ_u/u_*	σ_v/u_*	σ_w/u_*
Nanjing suburban area (this study)	Height 2 m above grass land	15 Nov–29 Dec 2007	3.73	3.49	1.62
Nanjing suburban area (Peng et al., 2008)	Pukou's tower layer at height 2 m	17 Feb–2 Mar 2006	2.15	2.15	1.18
Nanjing city center (Peng et al., 2008)	2.2 m above the roof (21 m)	17 Feb–2 Mar 2006	1.95	1.95	1.2
Nanjing suburban area (Xu et al., 1997)	Tower with a height 164m in Baguazhou	10–16 May 1990	2.3	2.1	1.35
Nanjing city center (Xu et al., 1997)	Tower with a height 50 m in campus	24–29 May 1990	2.46	2.15	1.23
Nanjing city center (Chen et al., 2000)	Tower with a height 50 m in campus	13–18 Jul 1998	2.16	1.62	1.28
Guanzhou city center (Xu et al., 1993)	7 m above the roof (28 m)	25 Jun–15 Jul 1988	2.32	1.89	1.47
Beijing urban area (Zhou et al., 2005)	Tower layer at height 47 m	19–29 Mar 2001, 11–25 Aug 2003	1.73	1.50	1.40
	Tower layer at height 120 m	19–29 Mar 2001, 11–25 Aug 2003	2.13	1.52	1.33
	Tower layer at height 280 m	19–29 Mar 2001, 11–25 Aug 2003	2.82	1.64	1.58
Chengdu Plain (Li et al., 2008)	Cropland	Feb–Apr 2007	2.00	2.10	1.20
Tibetan Plateau (Li et al., 2008)	Alm	Feb–Apr 2007	4.30	4.10	1.00
Tibetan Plateau (Bian et al., 2001)	Alp canyon	May–Jun 1998	3.45	3.15	1.30
Tibetan Plateau (Liu and Hong, 2000)	Flat surface	Jun–Jul 1998	3.21	2.69	1.46
Sublette, KS (Mahrt et al., 1998)	Plains	Mar 1995	2.45	1.90	1.25
Lander, BC (Mahrt et al., 1998)	Plains	Mar 1995	2.20	1.90	1.40
Beach Island, SC (Mahrt et al., 1998)	Plains	Mar 1995	2.30	1.90	1.35
Erie, CO (Mahrt et al., 1998)	Rough terrain	Mar 1995	2.65	2.00	1.20
Mountain (Mahrt et al., 1998)	Rough terrain	Mar 1995	3.50	3.80	1.24
(Panofsky and Dutton, 1984)	Flat surface		2.39	1.92	1.25

terrain around the observational site has little impact on vertical turbulences but has a great impact on horizontal turbulent motions. From Table 1 it can be concluded that the values of dimensionless standard deviations increase with increasing altitude and surface roughness. However, it is difficult to make a quantitative analysis because of the difference of the underlying surface, season, and the height of the sensor. In this experiment, the observation site was selected at an open suburban area, and the instruments were mounted at 2.0 m above ground level. These two factors led to large surface roughness. This may explain the large dimensionless standard deviations in Nanjing.

3.2 *Dimensionless turbulent kinetic energy (**TKE**)*

Turbulent kinetic energy (TKE)

$$e = \frac{1}{2}(\overline{u'^2} + \overline{v'^2} + \overline{w'^2}) = \frac{1}{2}\left(\sigma_u^2 + \sigma_v^2 + \sigma_w^2\right)$$

is a measure of turbulent intensity and larger value of TKE indicates a greater intensity of the microscale turbulence. For convenience, dimensionless TKE (e/u_*^2) is introduced by referring to the dimensionless standard deviations of velocity components. The relation between dimensionless TKE (e/u_*^2) and stability parameter z'/L is plotted in Fig. 3; it can be observed from the figure that the variation of TKE with stability exhibits a similar characteristic in comparison with dimensionless velocity standard deviations, i.e., it conforms to the 1/3 power law in both stable and unstable stratification. Their optimum similarity functions are as follows:

$$e/u_*^2 = \begin{cases} 12.85\,(1 + 51.49z'/L)^{1/3}\,, z'/L > 0 \\ 12.85\,(1 - 46.85z'/L)^{1/3}\,, z'/L < 0 \end{cases} \quad (3)$$

3.3 *Turbulence characteristics in different weather*

The field observational experiment was performed in November–December, a transition time period from autumn to winter seasons, when cold activities are frequent and fogs are also the most frequent of the year. To analyze the turbulence characteristics under different weather conditions, the observational data were first sorted by daily mean cloud cover into four categories: clear sky (cloud cover <30%), cloudy (cloud cover between 60% and 80%), overcast (cloud cover >90%), and fog days (i.e., where fogs lasted for >6 h in one day). Data for partial days, i.e., when the time period of usable data was <12 h, were removed from the observation record.

Table 2. Dimensionless standard deviations of velocity components and dimensionless TKE in near-neutral stratification in different weather.

	σ_u/u_*	σ_v/u_*	σ_w/u_*	e/u_*^2
Clear sky	3.778	3.696	1.594	16.579
Cloudy	3.665	3.423	1.648	14.823
Overcast	3.730	3.494	1.617	16.093
Fog day	5.383	4.728	1.545	30.327

The neutral, stable, and unstable stratification were defined in this study as $-0.1 \leqslant z'/L \leqslant 0.1$, $z'/L > 0.1$ and $z'/L < -0.1$, respectively. The dimensionless standard deviations of three wind components and dimensionless TKE under neutral stratification in different weather were analyzed (Table 2). From Table 2 it can be seen that for various weather conditions the order $\sigma_u/u_* > \sigma_v/u_* > \sigma_w/u_*$ is valid. Under different weather conditions the deviations of horizontal wind component and dimensionless TKE were the largest in fog days, the next largest in clear-sky days, and the smallest in cloudy days. Conversely, the vertical wind component was largest in cloudy days, the next largest in overcast days, and the smallest in fog days. The horizontal wind component and TKE in fog days were obviously larger than other counterparts; this suggests that the horizontal turbulence was very strong; it is propitious to the horizontal exchange of moisture and heat.

3.4 *Drag coefficient*

Drag coefficient $C_{\mathrm{D}} = u_*^2/\overline{u}^2$ reflects the roughness state of underlying surface. Many studies on C_{D} have been performed in China and other countries. Davidson (1974) summarized the C_{D} in plains areas and pointed out that C_{D} usually ranged from 1.4×10^{-3} to 2.6×10^{-3}. Zhou et al. (1998) analyzed the surface-layer observation data of the second Tibetan Plateau Experiment of Atmospheric Sciences (TIPEX) at Gaize, Dangxiong, and Changdu during May–July 1998, and reported that C_{D} ranged between 10^{-3} and 10^{-2}. Yao (2005) analyzed the variation of C_{D} with height of instrument in Beijing, and found that C_{D} increased dramatically with the lowering height, and the value of C_{D} could reach 10^0 near the surface. C_{D} is affected by viscous drag and form drag; the value of C_{D} increases with the increasing surface layer roughness or lowering instrument height. Figure 4 shows the C_{D} values derived from the sonic anemometer-thermometer observations in the surface layer in the northern Nanjing suburban area. From the figure it can be seen that C_{D} tends to slightly increase when z'/L transits from negative value to positive value. In neutral stratification, the C_{D} mainly concentrates in the range of 0.005 to 1, especially in the vicinity of

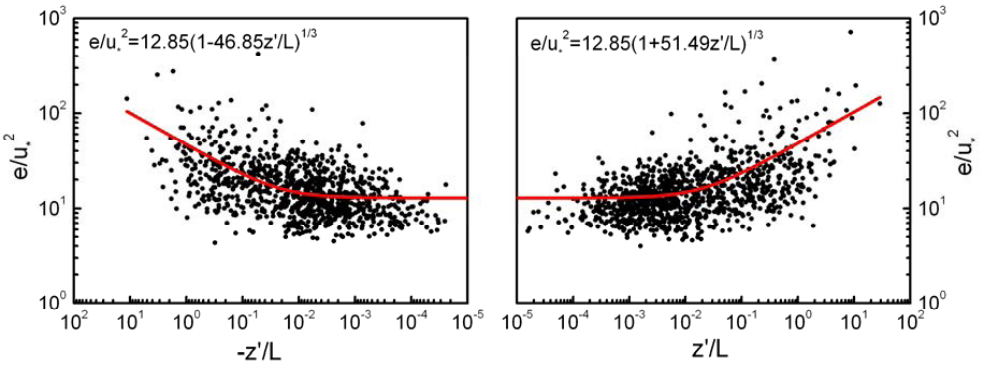

Fig. 3. Dimensionless TKE as a function of stability.

0.01. Therefore, the $C_{\rm D}$ values at the northern Nanjing suburban measurement site in the observation period are comparable with Beijing but are obviously higher than at other reported areas, and are approximately one order larger in magnitude than the reported plains areas. The value of $C_{\rm D}$ at the northern Nanjing suburban area during the observation period is higher than at other reported plains and plateau areas for three probable reasons. First, the roughness of underlying surface in a suburban area is much larger than in an open field. Second, in spite of the fact that the observation site is located in an open suburban area, the form drag generated by pressure gradients upwind and downwind of buildings and trees is relatively large. Third, the low height (2.0 m) of the instrument can also contribute to the large $C_{\rm D}$, as shown by results in Beijing (Yao, 2005).

3.5 *Dimensionless standard deviations of temperature*

Figure 5 shows the plots of the variation of dimensionless temperature standard deviation with z'/L.

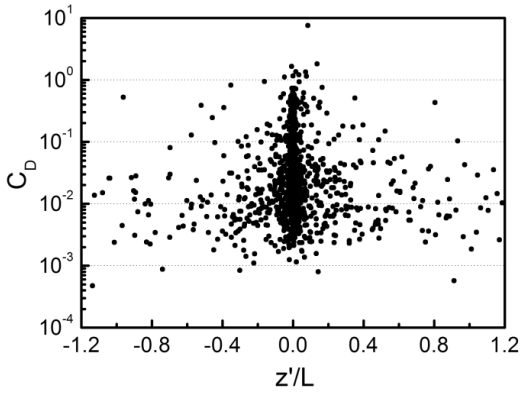

Fig. 4. Drag coefficient as a function of stability.

Their fitted optimum similarity functions in unstable and stable stratification are:

$$\sigma_T/|T_*| = \begin{cases} 5.98\,(-z'/L)^{-1/3}\,, & z'/L < 0 \\ 0.82\,(z'/L)^{-2/3}\,, & z'/L > 0 \end{cases}, \qquad (4)$$

where $T_* = -\overline{w'T'}/u_*$ is the characteristic temperature.

Figure 5 shows that, in unstable and stable stratification, $\sigma_T/|T_*|$ decreases with increasing $|z'/L|$ with an approximate "$-1/3$" and "$-2/3$" slope, respectively. And $\sigma_T/|T_*|$ changes slightly when $|z'/L| > 0.1$. This is because in stable stratification, thermal turbulences are suppressed, therefore the heat exchange between land and atmosphere is slow; whereas in unstable stratification, upper and lower air mix adequately, and the distribution of temperature vertically tends to be homogeneous. Mahrt et al. (1998) analyzed turbulence observations at heights of 3 m and 10 m in stable stratification conditions and found that $\sigma_T/|T_*|$ increased with increasing z'/L when z'/L<0.06 and decreased with increasing stability afterz'/L>0.06. This is thought to occur because $\overline{w'T'}$ increases with increasing stability when z'/L>0.06, considering that $\overline{w'T'}$ is negative in the stable regime, meaning that the absolute value of $\overline{w'T'}$ decreases with increasing stability. Similarly, $\overline{w'T'}$ decreases with increasing stability when z'/L<0.1 and increases with increasing stability after z'/L>0.1 (Fig. 2b). But $\sigma_T/|T_*|$ changes slightly when $|z'/L|$>0.1, because both the absolute value of $\overline{w'T'}$ and u_* decrease with increasing stability after z'/L>0.1. This indicates that dynamic and thermal processes near the underlying surface in the northern Nanjing suburban area may differ from those in plains areas, which leads to different trends of change in $\sigma_T/|T_*|$ with stability.

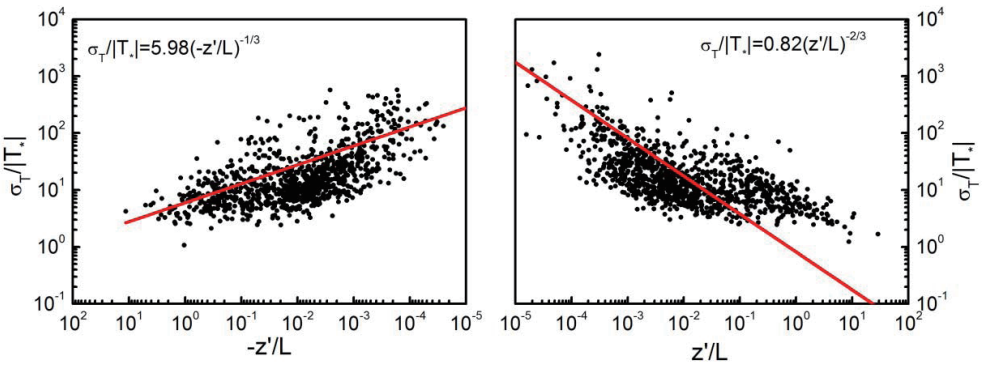

Fig. 5. Dimensionless temperature standard deviation as a function of stability.

4. Summary

The turbulent characteristics in the northern Nanjing suburban area were obtained using observational data. σ_u/u_*, σ_v/u_*, and σ_w/u_* in the surface layer in stable ($z'/L>0.1$), neutral ($-0.1\leqslant z'/L\leqslant 0.1$), and unstable ($z'/L<-0.1$) stratification in the Najing suburban area all follow the 1/3 power law; and dimensionless TKE in unstable and stable stratification both obey the 1/3 power law. Different characteristics of the underlying surface mainly impact dimensionless standard deviations of horizontal components of wind velocity, but they may also slightly impact those of the vertical component. The dimensionless standard deviations of wind components and dimensionless TKE in the boundary layer of the northern Nanjing suburban area are remarkably affected by different weather conditions. The order $\sigma_u/u_*>\sigma_v/u_*>\sigma_w/u_*$ is valid in neutral regime under various weather conditions; the deviations of horizontal wind component and dimensionless TKE present fog day > clear sky > overcast > cloudy; the trend of the vertical wind component is reverse.

The value of drag coefficient at the Nanjing suburban measurement site during the observation period is obviously higher than at other reported plains and plateau areas, and it is approximately one order larger in magnitude than that reported in plains areas. Dimensionless standard deviation of temperature declines with the increase of $|z'/L|$ with an approximate "$-1/3$" slope in unstable stratification and "$-2/3$" slope in stable stratification. The different change trends of $\sigma_T/|T_*|$ with stability indicate that dynamic and thermal processes near the underlying surface in the northern Nanjing suburban area may differ from those in plains areas.

Acknowledgements. Funding for this work was mainly provided by the Natural Science Fund for Universities in Jiangsu Province (Grant No. 08KJA170002), the Meteorology Fund of the Ministry of Science and Technology [Grant No. GYHY(QX) 2007-6-26], the National Natural Science Foundation of China (Grant No. 40775012) , and the National Key Technology R&D Program (Grant No. 2008BAC48B01), the Qing-Lan Project for Cloud-Fog-Precipitation-Aerosol Study in Jiangsu Province, the Graduate Student Innovation Plan for the Universities of Jiangsu Province (Grant No. CX10B_292Z), and a Project Funded by the Priority Academic Development of Jiangsu Higher Education Institutions.

REFERENCES

Argüeso, D., J. M. Hidalgo-Munoz, S. R. Gámiz-Fortis, M. J. Esteban-Parra, J. Dudhia, and Y. Castro-Díez, 2011: Evaluation of WRF parameterizations for climate studies over Southern Spain using a multi-step regionalization. *J. Climate*, **24**(21), 5633–5651, doi: 10.1175/JCLI-D-11-00073.1.

Bian, L., L. Lu, Y. Cheng, and C. Lu, 2001: Turbulent measurement over the southeastern Tibetan Plateau. *Journal of Applied Meteorological Science*, **12**(1), 1–13. (in Chinese)

Braun, S. A., and W. K. Tao, 2000: Sensitivity of high-resolution simulations of hurricane Bob (1991) to planetary boundary layer parameterization. *Mon. Wea. Rev.*, **128**, 3941–3961.

Carson, D. J., and P. J. R. Richards, 1978: Modelling surface turbulent fluxes in stable conditions. *Bound.-Layer Meteor.*, **14**, 67–81.

Caughey, S. J., J. C. Wyngaard, and J. C. Kaimal, 1979: Turbulence in the evolving stable boundary layer. *J. Atmos. Sci.*, **36**, 1041–1052.

Chen, M., Z. Li, and Q. Wang, 2000: A study of turbulence structure and turbulence transfer characteristic in the surface-layer at Nanjing city. *Scientia Meteorological Sinica*, **20**, 111–119. (in Chinese)

Cheng, Y., M. B. Parlange, and W. Brutsaert, 2005: Pathology of Monin-Obukhov similarity in the stable boundary layer. *J. Geophys. Res.*, **110**, D06101,

doi: 10.1029/2004JD004923.

Davidson, K. L., 1974: Observational results on the influence of stability and wind-wave coupling on momentum transfer and turbulence fluctuations over ocean waves. *Bound.-Layer Meteor.*, **6**, 305–332.

Deardorff, J. W., 1970: A three-dimensional numerical investigation of the idealized planetary boundary layer. *Geophys. Fluid Dyn.*, **1**, 377–410.

Dias, N. L., and W. Brutsaert, 1996: Similarity of scalars under stable stratification. *Bound.-Layer Meteor.*, **80**, 355–373.

Dias, N. L., W. Brutsaert, and M. L. Wesley, 1995: z-Less stratification under stable conditions. *Bound.-Layer Meteor.*, **75**, 175–187.

Eugster, W., and W. Senn, 1995: A cospectral correction model for measurement of turbulent NO_2 flux. *Bound.-Layer Meteor.*, **74**(4), 321–340.

Foken, T., 2006: 50 years of the Monin–Obukhov similarity theory. *Bound.-Layer Meteor.*, **119**, 431–447, doi: 10.1007/s10546-006-9048-6.

Foken, T., and B. Wichura, 1996: Tools for quality assessment of surface-based flux measurements. *Agricultural and Forest Meteorology*, **78**(1), 83–105.

Forrer, J., and M. W. Rotach, 1997: On the turbulence structure in the stable boundary layer over the Greenland ice sheet. *Bound.-Layer Meteor.*, **85**, 111–136.

Grimmond, C. S. B., and T. R. Oke, 1999: Aerodynamic properties of urban areas derived from analysis of urban form. *J. Appl. Meteor.*, **38**, 1262–1292.

Grimmond, C. S. B., and T. R. Oke, 2002: Turbulent heat fluxes in urban areas: Observations and a local-scale urban meteorological parameterization scheme (LUMPS). *J. Appl. Meteor.*, **41**, 792–810.

Hammerle, A., A. Haslwanter, M. Schmitt, M. Bahn, U. Tappeiner, A. Cernusca, and G. Wohlfahrt, 2007: Eddy covariance measurements of carbon dioxide, latent and sensible energy fluxes above a meadow on a mountain slope. *Bound.-Layer Meteor.*, **122**(2), 397–416, doi: 10.1007/s10546-006-9109-x.

Hartogensis, O. K., and H. A. R. De Bruin, 2005: Monin–Obukhov similarity functions of the structure parameter of temperature and turbulent kinetic energy dissipation rate in the stable boundary layer. *Bound.-Layer Meteor.*, **116**, 253–276, doi: 10.1007/s10546-004-2817-1.

Hicks, B. B., 1976: Wind profile relationships from Wangara Experiment. *Quart. J. Roy. Meteor. Soc.*, **102**, 535–551.

Hill, K. A., and G. M. Lackmann, 2009: Analysis of idealized tropical cyclone simulations using the Weather Research and Forecasting model: Sensitivity to turbulence parameterization and grid spacing. *Mon. Wea. Rev.*, **137**, 745–765, doi: 10.1175/2008MWR2220.1.

Hiller, R., M. J. Zeeman, and W. Eugster, 2008: Eddy-covariance flux measurements in the complex terrain of an Alpine Valley in Switzerland. *Bound.-Layer Meteor.*, **127**, 449–467, doi: 10.1007/s10546-008-9267-0.

Howell, J. F., and J. Sun, 1999: Surface-layer fluxes in stable conditions. *Bound.-Layer Meteor.*, **90**, 495–520.

Kaimal, J. C., J. C. Wyngaard, D. A. Hauger, O. R. Cote, Y. Izumi, S. J. Caughey, and C. J. Readings, 1976: Turbulence structure in the convective boundary layer. *J. Atmos. Sci.*, **33**, 2152–2169.

Li, Y., Y. Li, and X. Zhao, 2008: The comparison and analysis of ABL observational data on the east edge of Tibetan Plateau and in Chengdu Plain II: Characteristics of turbulence in the surface layer. *Plateau and Mountain Meteorology Research*, **28**(3), 8–14. (in Chinese)

Liu, H., and Z. Hong, 2000: Turbulence characteristics of surface layer in the Gaize region of Tibetan Plateau. *Scientia Atmospheric Sinica*, **24**, 289–300. (in Chinese)

Liu, H., Z. Hong, and Q. Li, 2002: Turbulent statistical characteristics over the urban surface. *Chinese J. Atmos. Sci.*, **26**, 173–181. (in Chinese)

Mahrt, L., 1999: Stratified atmospheric boundary layers. *Bound.-Layer Meteor.*, **90**, 375–396.

Mahrt, L., J. Sun, W. Blumen, T. Delany, and S. Oncley, 1998: Nocturnal boundary-layer regimes. *Bound.-Layer Meteor.*, **88**, 255–278.

Malhi, Y. S., 1995: The significance of the dual solutions for heat fluxes measured by the temperature fluctuation method in stable conditions. *Bound.-Layer Meteor.*, **74**, 389–396.

Martilli, A., 2002: Numerical study of urban impact on boundary layer structure: Sensitivity to wind speed, urban morphology, and rural soil moisture. *J. Appl. Meteor.*, **41**, 1247–1266.

Masson, V., C. S. B. Grimmond, and T. R. Oke, 2002: Evaluation of the town energy balance (TEB) scheme with direct measurements from dry districts in the cities, *J. Appl. Meteor.*, **41**, 1011–1026.

Monin, A. S., and A. M. Obukhov, 1954: Basic laws of turbulent mixing in the ground layer of the atmosphere. *Trudy Geofizicheskogo Instituta, Akademiya Nauk SSSR*, **24**(151), 163–187.

Nieuwstadt, F. T. M., 1984a: The turbulent structure of the stable, nocturnal boundary layer. *J. Atmos. Sci.*, **41**, 2202–2216.

Nieuwstadt, F. T. M., 1984b: Some aspects of the turbulent stable boundary layer. *Bound.-Layer Meteor.*, **30**, 31–55.

Pahlow, M., M. B. Parlange, and F. P. Agel, 2001: On Monin-Obukhov similarity in the stable atmospheric boundary layer. *Bound.-Layer Meteor.*, **99**, 225–248.

Panofsky, H. A. and J. A. Dutton, 1984: *Atmospheric Turbulence.* John Wiley and Sons, New York, 397pp.

Panofsky, H. A., H. Tennekes, D. H. Lenschow, and J. C. Wyngaard, 1977: The characteristics of turbulent velocity components in the surface layer under convective conditions. *Bound.-Layer Meteor.*, **11**, 355–361.

Peng, J., X. Wu, Z. Jiang, and H. Liu, 2008: Comparison of turbulent characters over urban and suburban

surface layer in Nanjing winter. *Journal of Nanjing Institute of Meteorology*, **31**(6), 871–878. (in Chinese)

Rotach, M. W., 1995: Profiles of turbulence statistics in and above on urban street canyon. *Atmos. Environ.*, **29**, 1473–1486.

Sharan, M., and S. G. Gopalakrishnan, 1999: A local parameterization scheme for σ_w under stable conditions. *J. Appl. Meteor.*, **38**, 617–622.

Simpson, I. J., G. W. Thurtell, H. H. Neumann, G. D. Hartog, and G. C. Edwards, 1998: The validity of similarity theory in the roughness sublayer above forests. *Bound.-Layer Meteor.*, **87**, 69–99.

Smedman, A., 1988: Observations of a multi-level turbulence structure in a very stable boundary layer. *Bound.-Layer Meteor.*, **44**, 231–253.

Sorbjan, Z., 1987: An examination of local similarity theory in the stably stratified boundary layer. *Bound.-Layer Meteor.*, **38**, 63–71.

Srinivas, C. V., R. Venkatesan, D. V. Bhaskar Rao, and D. Hari Prasad, 2007: Numerical simulation of Andhra severe cyclone (2003): Model sensitivity to the boundary layer and convection parameterization. *Pure Appl. Geophys.*, **164**, 1465–1487, doi: 10.1007/s00024-007-0228-1.

Stull, R. B., 1988: *An Introduction to Boundary Layer Meteorology.* Kluwer Academic Publishers, Dordrecht, 666pp.

Vickers, D., and L. Mahrt, 1997: Quality control and flux sampling problems for tower and aircraft data. *J. Atmos. Oceanic Technol.*, **14**(3), 512–526.

Wang, J., W. Wang, Y. Ao, F. Sun, and S. Wang, 2007: Turbulence flux measurements under complicated conditions. *Advances in Earth Science*, **22**(8), 791–797. (in Chinese)

Webb, E. K., G. I. Pearman, and R. Leuning, 1980: Correction of flux measurements for density effects due to heat and water vapor transfer. *Quart. J. Roy. Meteor. Soc.*, **106**(447), 85–100.

Wilson, K., A., and Coauthors, 2002: Energy balance closure at fluxnet sites. *Agricultural and Forest Meteorology*, **113**, 223–243.

Xu, Y., C. Zhou, and Z. Li, 1997: Turbulent structure and local similarity in the tower layer over the Nanjing area. *Bound.-Layer Meteor.*, **82**, 1–21.

Xu, Y., C. Zhou, Z. Li, and Z. Li, 1993: Microstructure and spectral characteristics of turbulence in the surface layer atmosphere over Guangzhou. *Scientia Atmospheric Sinica*, **17**, 338–348. (in Chinese)

Yao, W., 2005: Characteristics of urban boundary lower layer turbulence dynamical structure and its effects in Beijing. PH. D. dissertation, Chinese Academy of Meteorological Sciences and Nanjing University of Information Science & Technology, 175pp.

Zhou, M., X. Xu, L. Bian, and J. Chen, 1998: Observational analysis and dynamic study of the boundary layer of the Qinghai-Xizang Plateau. Chinese Meteorological Press, Beijing, 125pp.

Zhou, M., W. Yao, X. Xu, and H. Yu, 2005: Vertical dynamic and thermodynamic characteristics of urban lower boundary layer and its relationship with aerosol concentration over Beijing. *Science China* (*D*), **48**(SuppII), 25–37. (in Chinese)

Zilitinkevich, S. S., and I. N. Esau, 2007: Similarity theory and calculation of turbulent fluxes at the surface for the stably stratified atmospheric boundary layer. *Bound.-Layer Meteor.*, **125**, 193–205, doi: 10.1007/s10546-007-9187-4.